Spin gating electrical current

C. Ciccarelli, L. P. Zârbo, A. C. Irvine, R. P. Campion, B. L. Gallagher et al.

Citation: Appl. Phys. Lett. **101**, 122411 (2012); doi: 10.1063/1.4752013
View online: http://dx.doi.org/10.1063/1.4752013
View Table of Contents: http://apl.aip.org/resource/1/APPLAB/v101/i12
Published by the American Institute of Physics.

Spin gating electrical current

C. Ciccarelli,[1] L. P. Zârbo,[2] A. C. Irvine,[1] R. P. Campion,[3] B. L. Gallagher,[3] J. Wunderlich,[2,4] T. Jungwirth,[2,3] and A. J. Ferguson[1,a)]
[1]*Cavendish Laboratory, University of Cambridge, CB3 0HE, United Kingdom*
[2]*Institute of Physics ASCR, v.v.i., Cukrovarnická 10, 162 53 Praha 6, Czech Republic*
[3]*School of Physics and Astronomy, University of Nottingham, Nottingham NG7 2RD, United Kingdom*
[4]*Hitachi Cambridge Laboratory, Cambridge CB3 0HE, United Kingdom*

(Received 23 July 2012; accepted 28 August 2012; published online 20 September 2012)

The level of the chemical potential is a fundamental parameter of the electronic structure of a physical system, which consequently plays an important role in defining the properties of active electrical devices. We directly measure the chemical potential shift in the relativistic band structure of the ferromagnetic semiconductor (Ga,Mn)As, controlled by changes in its magnetic order parameter. Our device comprises a non-magnetic aluminum single electron channel capacitively coupled to the (Ga,Mn)As gate electrode. The chemical potential shifts of the gate are directly read out from the shifts in the Coulomb blockade oscillations of the single electron transistor. The experiments introduce a concept of spin gating electrical current. In our spin transistor spin manipulation is completely removed from the electrical current carrying channel. © *2012 American Institute of Physics*. [http://dx.doi.org/10.1063/1.4752013]

Magnetization dependent chemical potential shifts in the relativistic band structure of magnetic materials have rarely been discussed in the scientific literature. This reflects the conceptual difficulty in describing the chemical potential shifts by quantitative theories, the lack of direct measurements of the effect, and the lack of proposals in which the phenomenon could open unconventional paths in microelectronic device designs. References 1 and 2 are among the few attempts to quantify chemical potential anisotropies with respect to the spin orientation in semiconductor and metal magnets using relativistic model Hamiltonian or full-potential density-functional band structure calculations. The theories could account for chemical potential shifts due to the distortion in the dispersion of the spin-orbit coupled bands but for principle reasons omit possible shifts of the vacuum level with respect to band edges, in other words, possible shifts in band line-ups in realistic heterostructure systems. In experiments reported to date, the magnetic materials have been integrated in a conventional design of a magneto-electronic device, i.e., embedded in the transport channel, and the chemical potential shifts could have been inferred only indirectly from the measured data.[1,3–8] In the work presented in this letter we address the above two basic experimental points by demonstrating direct measurements of chemical potential shifts in a spin-orbit coupled ferromagnet and by demonstrating a spintronic device which operates without spin currents, i.e., a functionality which goes beyond the common concepts of spintronics.

Spin phenomena and functionalities have been incorporated in the transport channel of single electron transistor SETs, both in the leads and/or in the island. Observed effects include spin accumulation on the island and large tunnelling magnetoresistances.[9] In particular, large magnetoresistances due to magneto-Coulomb oscillations[3–5] or Coulomb blockade anisotropic magnetoresistance (AMR),[1,6,7] associated with chemical potential effects, have been observed in single electron transistors with ferromagnetic leads or islands. These studies showed that transport through the channel can be controlled by shifts of the chemical potentials at individual components of the SET channel, induced by the Zeeman coupling to the external magnetic field[3–5] or by magnetization rotation and relativistic spin-orbit coupling.[1,6,7] The latter phenomenon can yield low-field hysteretic magnetoresistances of huge magnitudes and, due to its origins in spin-orbit coupling, is related to AMR in conventional ohmic[10,11] or tunneling[12] devices. The chemical potential anisotropy has also been observed in (Ga,Mn)As tunnel devices.[8]

Our SET has a micron-scale aluminium island separated by aluminium oxide tunnel junctions from source and drain leads (Fig. 1(a)). The aluminium is lightly doped with manganese to suppress superconductivity in our low-temperature (300 mK) measurements. The SETs are fabricated on top of epitaxially grown (Ga,Mn)As layers, which are electrically insulated from the SET by an alumina dielectric, and act as a spin-back-gate to the SET. We choose (Ga,Mn)As for the gate electrode due to its well established relativistic magnetic anisotropy characteristics.[13,14] The low total capacitance ($C_\Sigma \sim 0.6$ fF) of the island to its leads and back-gate yields a single-electron charging energy ($E_c = e^2/2C_\Sigma$) of $\sim 100\,\mu$eV.

By sweeping the externally applied potential to the SET gate (V_g) we obtain the conductance oscillations that characterize Coulomb blockade, as shown in Fig. 1(b). In samples with magnetic gates we see a shift of these oscillations by an applied saturating magnetic field which rotates the magnetization in the (Ga,Mn)As gate. In Fig. 1(b) we show measurements for the in-plane ($\Phi = 90^\circ$) and for the perpendicular-to-plane ($\Phi = 0^\circ$) directions of magnetization. Alternatively, we plot in Fig. 1(c) the channel conductance as a function of the magnetization angle Φ for a fixed external potential V_g applied to the gate. The oscillations in Φ seen in Fig. 1(c) are of comparable amplitude as the oscillations in V_g in Fig. 1(b).

Due to the spin-orbit coupling, the band structure of (Ga,Mn)As is perturbed when its magnetization **M** is rotated.

a)Electronic mail: ajf1006@cam.ac.uk.

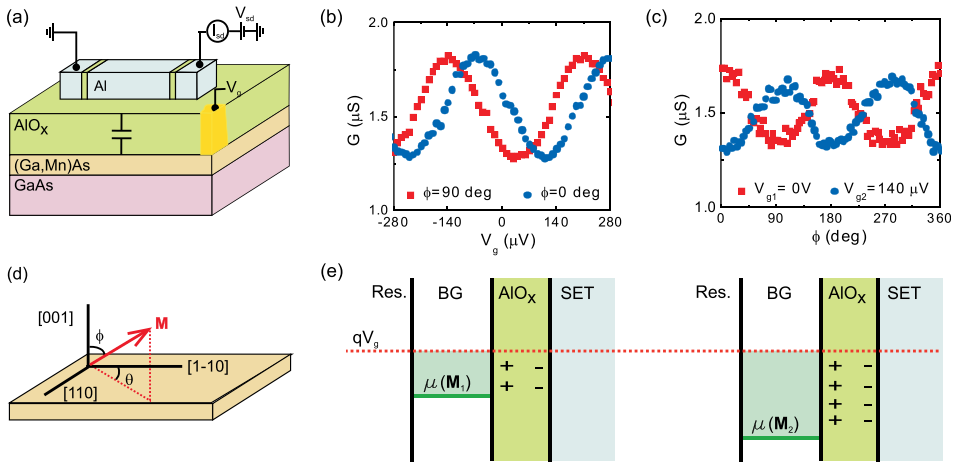

FIG. 1. (a) Schematic showing our SET channel separated by AlO_x dielectric from the ferromagnetic (Ga,Mn)As back-gate. The SET comprises Al leads and island, and AlO_x tunnel barriers. (b) Coulomb oscillations for the SET on $(Ga_{0.97},Mn_{0.03})As$ for two different polar angles Φ of the magnetization. (c) Magneto-Coulomb oscillations shown by the same SET by varying the angle of magnetization for two different gate voltages. Measurements were performed using a low frequency lock-in technique with excitation voltage 20 μV and zero dc bias. (d) Magnetization vector with respect to (Ga,Mn)As crystal axes. (e), Schematic explaining the spin gating phenomenon: reorientation of the magnetization from $\mathbf{M}_1$ to $\mathbf{M}_2$ causes a change in the chemical potential of the (Ga,Mn)As back-gate (BG). This causes charge to flow onto the back-gate from the reservoir (Res.). The net effect is to alter the charge on the back-gate and therefore the SET conductance. We show a decrease in hole chemical potential μ between $\mathbf{M}_1$ and $\mathbf{M}_2$. The externally applied electrochemical potential on the gate $\mu_{ec} = qV_g$ is held constant.

One consequence is a shift of the chemical potential, which in itself does not yield a response of the SET. However, the back-gate is attached to a charge reservoir so any change in the internal chemical potential of the gate causes an inward, or outward, flow of charge in the gate, as illustrated in Fig. 1(e). This change in back-gate charge offsets the Coulomb oscillations (Fig. 1(b)) and changes the conductance of the transistor channel for a fixed external potential applied to the gate (Fig. 1(c)). Any magneto-Coulomb effect from a **M**-dependent change in the depletion region at the surface[15] is ruled out: this would lead to the shift in Coulomb oscillations being dependent on the magnitude of the gate voltage.

We now display the full experimental data sets for out-of-plane magnetization rotations in a saturating magnetic field in the case of a ferromagnetic p-type $(Ga_{0.97},Mn_{0.03})As$ gate (Fig. 2(a)). We fit a sinusoid to the Coulomb oscillations and extract the resulting gate-voltage offset (ΔV_g) as a function of the magnetization angle. A positive value of ΔV_g means that, for a fixed gate voltage, holes leave the gate, which can be attributed to an increased hole chemical potential, $\Delta\mu = q\Delta V_g$. It is important to note that in the case of the ferromagnetic gate no capacitance scaling factors are required and the chemical potential shift may be directly read off as a shift in gate voltage. This removes a source of systematic error, present in all previous experiments on the magneto-Coulomb effect[3–5] or chemical potential anisotropy,[1,6–8] where the gate voltage shift must be scaled due to the presence of a capacitive divider.

The anisotropy of $\Delta\mu$ for out-of-plane rotation of **M** has a uniaxial symmetry ($\Delta\mu^u_\Phi = 81\,\mu$eV) (Fig. 2(b)), whereas the in-plane rotation anisotropy is predominantly uniaxial ($\Delta\mu^u_\theta = 30\,\mu$eV) with a small cubic component ($\Delta\mu^c_\theta = 6\,\mu$eV) (Fig. 2(c)). The $\Delta\mu$ anisotropy is greater for the out-of-plane rotation and causes a shift in the Coulomb oscillations by a quarter of a period. We also measured SETs with a $(Ga_{0.94},Mn_{0.06})As$ back-gate. The magnitude of both the out-of-plane rotation ($\Delta\mu^u_\Phi = 144\,\mu$eV) and the in-plane

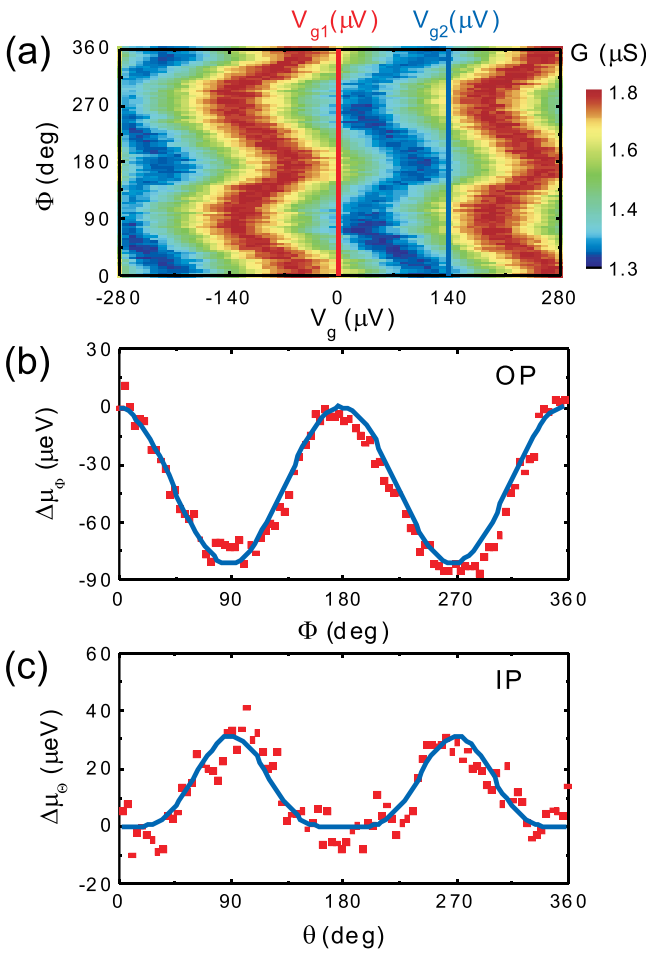

FIG. 2. (a) SET conductance measurements for azimuthal angle $\theta = 0$ as a function of the out-of-plane polar angles Φ of the $(Ga_{0.97},Mn_{0.03})As$ magnetization and of the gate voltage. The magnetization is rotated by a 1 T magnetic field. The two lines represent the gate voltage offsets for the data shown in Fig. 1(c). (b) $(Ga_{0.97},Mn_{0.03})As$ hole chemical potential shift ($\Delta\mu_\Phi = \mu(\Phi) - \mu(\Phi = 0)$) for the out-of-plane magnetization rotation, inferred from measurements in (a). (c) $(Ga_{0.97},Mn_{0.03})As$ hole chemical potential shift ($\Delta\mu_\theta = \mu(\theta) - \mu(\theta = 0)$) for the in-plane magnetization rotation.

rotation ($\Delta\mu_\theta^u = 46\,\mu$eV) uniaxial anisotropies increase in the sample with higher Mn concentration while the in-plane cubic anisotropy component is negligibly small in the ($Ga_{0.94}$,$Mn_{0.06}$)As sample. The chemical potential anisotropy constants are consistent between samples fabricated from the same MBE grown wafers. This is because the spin gating phenomenon measures the properties of the material surface (over a $\sim\mu m^2$ area in our sample) rather than a specific nanodevice.

We repeated field rotation measurements for different values of the saturating field, observing only a weak dependence of the $\Delta\mu$ anisotropy components on the field magnitude (Fig. 3(a)). This confirms that the origin of the observed spin-gating is the anisotropy of the chemical potential in the ferromagnetic gate with respect to the magnetization orientation (recall that the effective g-factor in the GaAs valence band has a negligible anisotropy[16]).

The chemical potential anisotropy origin of the observed spin-gating effect is confirmed by microscopic calculations based on the $\mathbf{k}\cdot\mathbf{p}$ kinetic-exchange model of (Ga,Mn)As (Refs. 17 and 18) (see Figs. 3(b) and 3(c)). We have calculated chemical potential anisotropies for the out-of-plane magnetization rotation assuming local Mn moment concentrations and lattice-matching growth strains corresponding to the measured (Ga,Mn)As samples. We consider one hole per Mn_{Ga} local moment (Mn_{Ga} is a single acceptor), as well as cases with partial hole depletion. The latter calculations were performed since the spin-gating experiments are sensitive to the partially depleted surface layer which has a width given by the hole screening length (a few nm).

In agreement with experiment, we find theoretical chemical potential anisotropies of the order of $10-100\,\mu$eV. The calculated enhancement of the chemical potential anisotropy with increasing local moment concentration and lattice-matching growth strain is also consistent with the enhanced spin-gating effect observed experimentally in the ($Ga_{0.94}$,$Mn_{0.06}$)As sample as compared to the ($Ga_{0.97}$,$Mn_{0.03}$)As sample. We also note that the increase in the higher Mn-doped sample of the measured and calculated chemical potential anisotropy for the out-of-plane rotation is consistent with the doping trends in the corresponding magnetocrystalline anisotropy coefficient of (Ga,Mn)As.[19] Similarly, the measured enhancement of the in-plane uniaxial component of the chemical potential anisotropy and the suppression of the cubic component in the higher Mn-doped sample is consistent with the corresponding magnetocrystalline anisotropy trends.[19] The microstructural origin of the in-plane uniaxial anisotropy component is not established and to capture this component one can, e.g., introduce an effective shear strain in the $\mathbf{k}\cdot\mathbf{p}$ Hamiltonian which breaks the [110]/[1-10] crystal symmetry.[19,20] The values of the shear strain required to reproduce the in-plane uniaxial magnetocrystalline anisotropy yield a corresponding chemical potential anisotropy of the order of $\sim 10-100\,\mu$eV, again consistent with our measured data. Similar to the established phenomenology of the spin-orbit coupling induced magnetocrystalline anisotropies, or ohmic and tunneling AMRs, the sign and magnitude of the chemical potential anisotropy is not strictly determined by the sign of the strain and by other symmetries of the crystal and may vary when changing the local moment or hole concentration

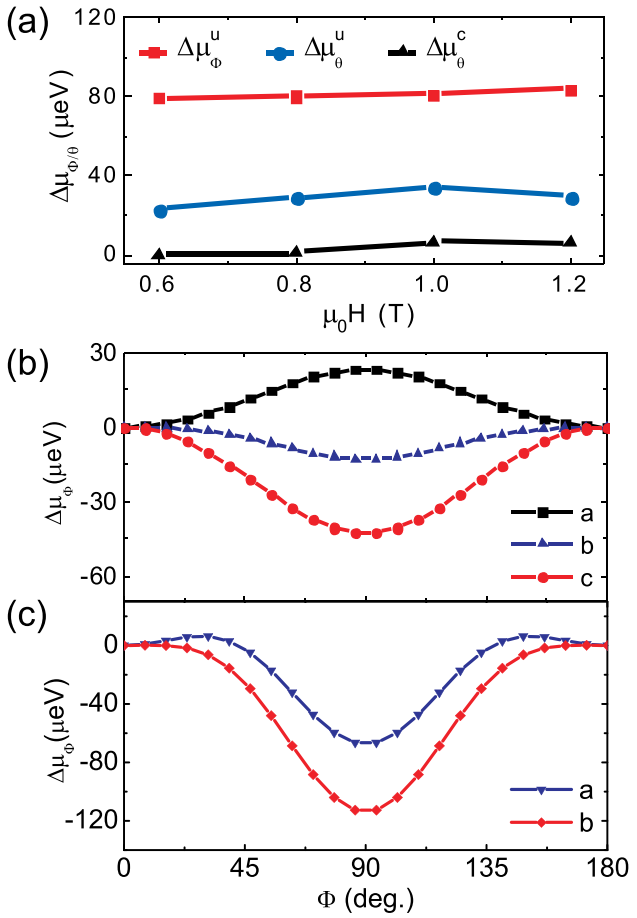

FIG. 3. (a) Experimental values for cubic and uniaxial contributions to the $\Delta\mu$ anisotropy, measured for different saturation fields, for the ($Ga_{0.97}$,$Mn_{0.03}$)As gate material. (b) Theoretical variations of the chemical potential with respect to the magnetization angle Φ for fixed Mn moment density $N_{Mn} = 4.4\times10^{20}$cm^{-3} (corresponding approximately to the measured sample with 3% nominal doping) and compressive growth strain $\epsilon_0 = -0.3\%$. The hole density $p = N_{Mn}$, $p = 0.4N_{Mn}$ and $p = 0.2N_{Mn}$ for curves a, b, and c, respectively. (c) Theoretical chemical potential anisotropies for $N_{Mn} = 8.8\times10^{20}$cm^{-3} (corresponding approximately to the measured sample with 6% nominal doping) and charge density $p = 0.2N_{Mn}$. The curve a is for the strain $\epsilon_0 = -0.3\%$ while curve b is for $\epsilon_0 = -0.5\%$.

in (Ga,Mn)As. We note that the agreement in the sign of the theoretical and experimental chemical potential anisotropy is obtained assuming partially depleted holes, consistent with the expected sensitivity in our device to the (Ga,Mn)As surface layer.

In ferromagnets, the chemical potential can also shift when the magnetization angle is fixed while the magnitude of the external magnetic field is varied. Performing a sweep of the magnetic field in the out-of-plane direction, we observe a nearly flat region followed by a decreasing chemical potential (Fig. 4(a)). The flat, low-field region occurs as **M** rotates from the in-plane easy axes to the out-of-plane direction. During the rotation of **M**, the **M**-orientation dependent and field-dependent contributions to $\Delta\mu$ nearly cancel. If we sweep the field along an in-plane easy axis, just the field-dependent $\Delta\mu$ is observed (Fig. 4(a)), consistent with the absence of **M** rotation.

At higher fields the decreasing chemical potential saturates and eventually increases (Fig. 4(b)). The decrease in chemical potential is due to an indirect mechanism in which

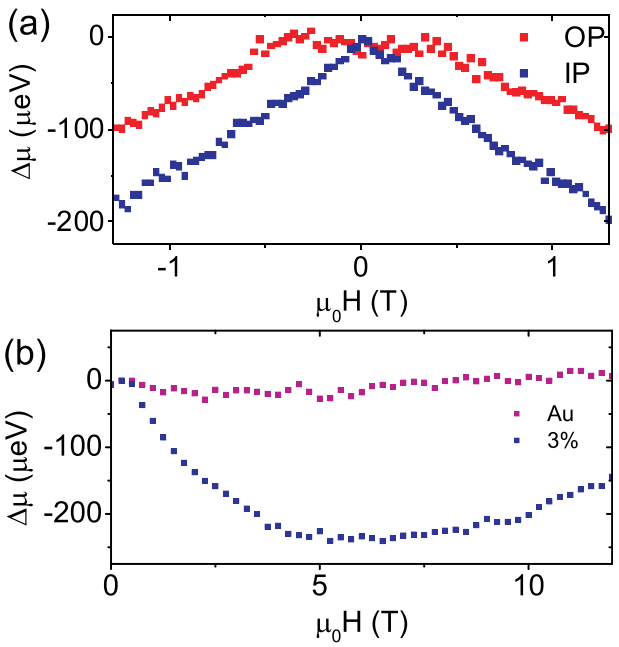

FIG. 4. (a) The chemical potential shift determined for out-of-plane and in plane easy axis sweeps of the magnetic field for the $(Ga_{0.97},Mn_{0.03})$As gate material. We refer the chemical potential to its zero field value. (b) The chemical potential shifts for a high field out of plane sweep for $(Ga_{0.97},Mn_{0.03})$As and also for a control sample with an Au gate.

the field acts on the hole bands via the kinetic-exchange coupling. We assume that apart from the ferromagnetic Mn moments being saturated by low magnetic fields corresponding to the magnetic anisotropy fields, a fraction of the Mn local moment magnetization is not fully saturated at the low-fields. Sweeping the field gradually polarizes these unsaturated moments which in our theoretical modeling corresponds to an increase of the effective concentration of the ferromagnetic local moments. The hole chemical potential decreases because the enhanced strength of the kinetic-exchange field due to the larger density of saturated local moments causes an enhancement of the spin-splitting of the hole bands. The field-dependent $\Delta\mu$ saturates at a value of $\sim$200 μeV. From the calculations we infer that such a shift corresponds to an effective $\sim$1% increase of the density of ferromagnetic local moments. The field-induced additional polarization of a small fraction of the local moment density can be readily expected for the studied samples but would be unobservable by standard magnetization measurements.

The mechanism for the increase in chemical potential at higher fields is the direct Zeeman coupling of the magnetic field to the hole bands. Similar to the above indirect mechanism, the sign of the chemical potential shift due to the Zeeman coupling is given by the sense in which the spin-splitting of the hole bands changes in the applied field. However, unlike the indirect mechanism, the Zeeman coupling reduces the spin-splitting of the hole bands which yields an increase of the chemical potential. The chemical potential increases with magnetic field because the magnetization of the local Mn moments and of the holes are antiparallel, a consequence of the p-d hybridization origin of the kinetic-exchange interaction.[13] To assess quantitatively the chemical potential shift due to the Zeeman coupling we performed the $\mathbf{k}\cdot\mathbf{p}$ kinetic-exchange calculations (including spin-orbit coupling) in the presence of the magnetic field directly acting on the hole bands. As expected, the calculated shift of the chemical potential is larger for larger hole depletion and in the more depleted case we obtain an increase of the chemical potential of the order of $\sim$10 μeV/T which is consistent with the experimental high-field trend seen in Fig. 4(b). The experimental data in Fig. 4(b) are shown for an out-of-plane field-sweep in $(Ga_{0.97},Mn_{0.03})$As, however, the same behaviour is observed for the in-plane sweep, consistent with the negligible anisotropy of the Zeeman effect in the 3D valence band of (Ga,Mn)As. A control SET with a Au gate (Fig. 4(b)) shows no systematic effect due to the magnetic field, and confirms that there is no significant magneto-conductance due to the aluminium-manganese alloy.

The spin-gating technique was employed to accurately measure the anisotropic, and isotropic, chemical potential phenomena in (Ga,Mn)As. However, this technique can be applied to catalogue these effects in other magnetic materials by the simple step of exchanging the gate electrode. We finish by emphasizing that our work comprises a spin transistor where the charge state of the device channel is sensitive to the spin state of its magnetic gate.

We acknowledge support from EU Grants FP7-214499 NAMASTE, FP7-215368 SemiSpinNet, ERC Advanced Grant, from Czech Republic Grants AV0Z10100521, KAN400100652, KJB100100802, and Preamium Academiae. A.J.F. acknowledges the support of a Hitachi research fellowship.

[1]J. Wunderlich, T. Jungwirth, B. Kaestner, A. C. Irvine, K. Y. Wang, N. Stone, U. Rana, A. D. Giddings, A. B. Shick, C. T. Foxon *et al.*, Phys. Rev. Lett. **97**, 077201 (2006).
[2]A. B. Shick, S. Khmelevskyi, O. N. Mryasov, J. Wunderlich, and T. Jungwirth, Phys. Rev. B **81**, 212409 (2010).
[3]K. Ono, H. Shimada, and Y. Ootuka, J. Phys. Soc. Jpn. **66**, 1261 (1997).
[4]M. M. Deshmukh and D. C. Ralph, Phys. Rev. Lett. **89**, 266803 (2002).
[5]S. J. van der Molen, N. Tombros, and B. J. van Wees, Phys. Rev. B **73**, 220406 (2006).
[6]M. Schlapps, T. Lermer, S. Geissler, D. Neumaier, J. Sadowski, D. Schuh, W. Wegscheider, and D. Weiss, Phys. Rev. B **80**, 125330 (2009).
[7]A. Bernand-Mantel, P. Seneor, K. Bouzehouane, S. Fusil, C. Deranlot, F. Petroff, and A. Fert, Nat. Phys. **5**, 920 (2009).
[8]M. Tran, J. Peiro, H. Jaffrès, J.-M. George, O. Mauguin, L. Largeau, and A. Lemaître, Appl. Phys. Lett. **95**, 172101 (2009).
[9]K. J. Dempsey and D. C. C. H. Marrows, Philos. Trans. R. Soc. A **369**, 3150 (2011).
[10]W. Thomson, Proc. R. Soc. London **8**, 546 (1857).
[11]T. McGuire and R. Potter, IEEE Trans. Magn. **11**, 1018 (1975).
[12]C. Gould, C. Rüster, T. Jungwirth, E. Girgis, G. M. Schott, R. Giraud, K. Brunner, G. Schmidt, and L. W. Molenkamp, Phys. Rev. Lett. **93**, 117203 (2004).
[13]T. Jungwirth, J. Sinova, J. Mašek, J. Kučera, and A. H. MacDonald, Rev. Mod. Phys. **78**, 809 (2006).
[14]*Semiconductors and Semimetals* (Elsevier, 2008), Vol. 82.
[15]K. Pappert, M. J. Schmidt, S. Hümpfner, C. Rüster, G. M. Schott, K. Brunner, C. Gould, G. Schmidt, and L. W. Molenkamp, Phys. Rev. Lett. **97**, 186402 (2006).
[16]R. Winkler, S. J. Papadakis, E. P. D. Poortere, and M. Shayegan, Phys. Rev. Lett. **85**, 4574 (2000).
[17]T. Dietl, H. Ohno, and F. Matsukura, Phys. Rev. B **63**, 195205 (2001).
[18]M. Abolfath, T. Jungwirth, J. Brum, and A. H. MacDonald, Phys. Rev. B **63**, 054418 (2001).
[19]J. Zemen, J. Kucera, K. Olejnik, and T. Jungwirth, Phys. Rev. B **80**, 155203 (2009).
[20]M. Sawicki, K.-Y. Wang, K. W. Edmonds, R. P. Campion, C. R. Staddon, N. R. S. Farley, C. T. Foxon, E. Papis, E. Kaminska, A. Piotrowska *et al.*, Phys. Rev. B **71**, 121302 (2005).